Ultrasound image resolution influences analysis of skeletal muscle composition

Michael T. Paris, MSc[1]

Kirsten E. Bell, PhD[1]

Egor Avrutin, MSc[1]

Marina Mourtzakis, PhD[1]

[1]Department of Kinesiology, University of Waterloo, Waterloo, ON, Canada.

Corresponding author: Marina Mourtzakis, PhD, Department of Kinesiology, University of Waterloo, 200 University Ave W, Waterloo, ON, N2L 3G1, Canada. Email: mmourtzakis@uwaterloo.ca. Phone: 519-888-4567, Ext 38459.

Word count: 3041

Display items: 2

Running head: Ultrasound image resolution

SUMMARY

INTRODUCTION: Analysis of muscle composition using ultrasound requires standardization of several equipment settings (i.e. gain). However, the influence of image resolution, which is altered by imaging depth, on measures of muscle composition is unknown.

METHODS: We analyzed rectus femoris muscle composition using ultrasound images captured from 32 males and females (aged 28±5 years) at depths of 9.0, 7.3, 5.9, and 4.7 cm. The transducer's orientation was fixed using a clamp during image acquisition to minimize movement. Across each image resolution, a region of interest encompassing the same anatomical area within the muscle was used for muscle composition analysis. Muscle composition was analyzed using a combination of first, second, and higher order texture features. Muscle composition agreement across image resolutions was evaluated using a one-way ANOVA and intraclass correlation coefficients (ICC).

RESULTS: Most muscle composition features displayed differences due to image resolution ($p<0.05$). ICCs demonstrated poor to good agreement across different image resolutions. In general, higher resolution images (i.e. shallower imaging depth) demonstrated better agreement (ICC>0.90) compared to lower resolution images.

CONCLUSIONS: Ultrasound image resolution influences muscle composition analysis. Image resolution should be fixed within and between individuals when evaluating muscle composition using ultrasound.

Keywords: ultrasound, skeletal muscle composition, muscle quality, echo intensity, echogenicity, body composition

INTRODUCTION

Skeletal muscle mass decreases with advancing age and several disease states (e.g. diabetes, cancer cachexia, and others) (Mitchell et al. 2012, Parry et al. 2015). The loss of skeletal muscle mass contributes to impairments in strength and physical function (Visser et al. 2005), however, these adverse changes cannot be entirely accounted for by changes in muscle mass (Goodpaster et al. 2006). The *composition* or *quality* of skeletal muscle tissue also deteriorates with age and disease (Frank-Wilson et al. 2018), and poor skeletal muscle composition (i.e. a high degree of inter- or intra-muscular adipose, or connective tissue infiltration) contributes to functional and metabolic impairments (Goodpaster et al. 2001). Measuring the infiltration of non-muscle tissue into skeletal muscle is challenging, and established reference methods are invasive (e.g. muscle biopsies), inaccessible (e.g. magnetic resonance imaging), or expose the individual to ionizing radiation (e.g. computed tomography). Ultrasound has emerged as a non-invasive, accessible, and safe modality that can provide surrogate measures of skeletal muscle composition (Paris and Mourtzakis 2016).

Muscle composition can be assessed from ultrasound images via texture analysis, a process by which mathematical features are used to describe the composition of tissues (Castellano et al. 2004). Several texture features may be used to characterize skeletal muscle composition, the most common of which is echo intensity. Echo intensity quantifies the average pixel intensity in a defined region of interest (ROI), with higher values (brighter images) indicating increased adipose and connective tissue infiltration (Harris-Love et al. 2014). Higher echo intensity has previously been shown to be associated with reduced strength (Wilhelm et al. 2014), functional capacity (Rech et al. 2014), and cardiorespiratory fitness (Cadore et al. 2012) in older adults. While echo intensity is a useful measure, more complex texture features may

have greater utility in characterizing skeletal muscle composition from ultrasound images. Echo intensity is considered a first order texture feature, as it only accounts for individual pixel intensities. Second and higher order texture features account for both pixel intensity as well as their spatial distribution (i.e. the relative location of each pixel throughout the muscle). These more complex texture features are emerging as suitable surrogates for skeletal muscle composition, which, compared with echo intensity, may better discriminate between males and females (Molinari et al. 2015), different muscle groups (Molinari et al. 2015), and neuromuscular diseases (König et al. 2015).

Given that ultrasound texture analysis of skeletal muscle composition is based on pixel intensity and spatial distribution, equipment settings that influence pixel intensity (i.e. gain, time-gain-compensation) must be standardized when comparing muscle composition across individuals. Within the existing literature, the majority of studies examining ultrasound muscle composition standardize these equipment settings for image acquisition. However, scanning depth is often changed between and within participants to optimize the field of view due to differences in muscle size or adipose tissue thickness. For example, a greater scanning depth is required to fully capture the anterior thigh muscles of a muscular or obese individual compared to a smaller-framed person. Altering the scanning depth changes the image resolution (i.e. number of pixels/area); but, the influence of image resolution on muscle composition texture analysis has yet to be comprehensively evaluated.

This study sought to examine the effect of image resolution on ultrasound measures of rectus femoris muscle composition (e.g. echo intensity and others) in healthy adults. We hypothesized that different image resolutions would alter muscle composition texture analysis, but that some features may be influenced to a lesser degree.

MATERIALS AND METHODS

Study design and participants – We conducted a prospective cross-sectional study which evaluated 32 healthy adults (≥ 18 years, n=16 males, n=16 females) recruited from the University of Waterloo campus community. Participants were instructed to refrain from strenuous lower body exercise for 24 h prior to their study visit. This study was approved by a human research ethics committee at the University of Waterloo. Written informed consent was obtained from all participants in accordance with established protocols for human research.

Anthropometry and landmarking – Weight and height were measured using a beam scale and stadiometer, respectively. Limb dominance was indicated by participant self-report. During landmarking, participants lay supine with their feet hip width apart and secured in position using a foot strap to prevent excessive internal or external hip rotation. We used a flexible tape measure and pen to mark the position 2/3 of the distance from the anterior superior iliac spine to the superior pole of the patella. We also measured the circumference of the thigh at this landmark. All measurements were made on the right leg.

Ultrasound image acquisition – Transverse images were taken using a real-time B-mode ultrasound imaging device (M-Turbo, SonoSite; Markham, ON) equipped with a multi-frequency linear array transducer (L38xi: 5-10 MHz). The imaging mode was set to "resolution" and the following settings were held constant throughout the study: gain (default), time-gain compensation (default), and dynamic range (50%). The transducer was generously coated with water-soluble transmission gel to minimize tissue depression. Previously, we have shown that minimal tissue compression is strongly correlated with appendicular lean tissue measured using dual-energy X-ray absorptiometry (Paris et al. 2017). Minimal compression was confirmed visually by ensuring that: 1) a layer of ultrasound gel remained between the probe and the skin

during imaging, and 2) the natural curvature of the skin, subcutaneous adipose tissue, and muscle tissue was maintained. The transducer was oriented in the medial-lateral plane to centre the rectus femoris and femur within the field of view and then tilted in the cranial-caudal plane to achieve the brightest femur bone echo (i.e. neutral transducer tilt). Once the correct orientation was achieved, the transducer was fixed in place using a flexible gooseneck clamp (**Figure 1**), and this position was maintained throughout the entire image acquisition process. Images of the rectus femoris were captured at discrete depths of 9.0, 7.3, 5.9, and 4.7 cm, which on our equipment correspond to image resolutions of 0.0234, 0.0189, 0.0153, and 0.0123 cm/pixel, respectively. All ultrasound images were saved in the Digital Imaging and Communications in Medicine (DICOM) format and transferred to a computer for analysis. Image resolution was determined from manufacturer information contained with the DICOM metadata.

Thickness measurements – For all participants, muscle and subcutaneous adipose tissue thicknesses were analyzed using the 9.0 cm depth images (ImageJ, version 1.52a, NIH; Bethesda, MD). Muscle thickness (which included both the rectus femoris and vastus intermedius) was obtained by measuring the perpendicular distance between the upper margin of the femur and the lower boundary of the rectus femoris fascia, as previously described (Paris et al. 2017)**.** Subcutaneous adipose tissue thickness was obtained by measuring the perpendicular distance between the superior border of the rectus femoris fascia and the inferior border of the skin at three locations: the medial, center, and lateral sections of the ultrasound image. The average of these three subcutaneous adipose tissue measurements was used in the analysis. A single trained analyst performed all thickness measures.

Muscle texture analysis – During texture analysis, placement of the ROI impacts muscle composition analysis (Caresio et al. 2014). Therefore, it is critical to select the same physical

area within the muscle of interest across all image resolutions. To minimize inconsistencies in ROI placement across images of differing resolutions, the initial ROI was manually selected in the 9.0 cm depth image and then automatically scaled to the remaining images (**Figure 2**). The ROI was selected to capture as much of the rectus femoris as possible, while excluding the surrounding muscle fascia. ROI scaling was successful for all participants across all depths, with the exception of one participant whose rectus femoris did not fully fit within the field of view at the 4.7 cm imaging depth.

At each image resolution, we evaluated several different texture features representing first, second, and higher order analysis. First order features account for individual pixel intensity, independent of spatial distribution. Second order and higher order features account for pixel intensities and the spatial relationships between pairs of pixels (second order) or three or more pixels (higher order). First order features were extracted from the ROI pixel intensity histogram and included mean echo intensity, kurtosis, and energy. Second order features were extracted from the grey-level co-occurrence matrix (GLCM), which encodes the frequency of pixel pair occurrences for a given intensity and spatial relationships (distance and angle) (Castellano et al. 2004). From the GLCM, measures of energy, correlation, and contrast were calculated and averaged across distances of 1 to 10 pixels and angles 0, 45, 90, and 135º (symmetric matrix) (Hall-beyer 2017). Higher order features were evaluated using local binary patterns (LBP), which Molinari et al. (2015) have demonstrated as being useful for muscle texture characterization. LBP evaluate the local spatial patterns of edges, points, and spots of an image. A LBP image, derived using a circular radius of 5 and 8 sampling points, was used to extract measures of energy for texture characterization (Molinari et al. 2015).

152 The mean echo intensity of muscle can range from 0 to 255 (black to white). Histogram
153 kurtosis represents the peakedness of the pixel intensity distribution. A value of 3 for kurtosis
154 represents a normal distribution, values above 3 indicate leptokurtic (sharper peak) and values
155 below 3 indicate platykurtic (flatter peak). Histogram energy, GLCM energy, and LBP energy
156 range from a minimum of 0 to a maximum of 1. GLCM correlation can range from -1 to 1. The
157 minimum value of GLCM contrast is 0, whereas the upper range is dependent on the bit depth of
158 the image. For an 8-bit ultrasound image, the range is from 0 to 65 025.

159 *Statistical analysis* – Differences between males and females were compared using independent
160 samples Student's t-tests. A repeated measures one-way ANOVA was used to test for differences
161 in muscle composition features between images obtained at the following depths: 9.0, 7.3, 5.9,
162 and 4.7 cm. Post hoc pairwise comparisons were performed using a Bonferroni correction. We
163 used intraclass correlations coefficients (ICC) to evaluate the agreement between muscle
164 composition texture features across different image resolutions. ICC (2,1) (Koo and Li 2016) for
165 absolute agreement were used to evaluate combined and all pairwise permutations of 9.0, 7.3,
166 5.9, and 4.7 cm depths. ICC values <0.5 indicate poor reliability; values between 0.5 – 0.75
167 indicate moderate reliability; values between 0.75 – 0.9 indicate good reliability; and values >0.9
168 indicate excellent reliability (Koo and Li 2016). All statistics analyses were performed using
169 SPSS (version 24, IBM, USA). Statistical significance was set as $p<0.05$.

170 **RESULTS**

171 On average, participants were normal weight according to BMI (24.4 ± 3.4 kg/m^2), and
172 84% (n=27) were right leg dominant. Compared with females (n=16), males (n=16) presented
173 with greater weight ($p<0.001$), height ($p<0.001$), BMI ($p=0.011$), and muscle thickness

174 ($p<0.001$), but lower adipose tissue thickness ($p=0.004$) (**Table 1**). The minimum imaging depth
175 required to fully visualize the rectus femoris in all participants was 5.9 cm (**Table 1)**.

176 We observed a significant effect of image resolution across all muscle composition
177 texture features (all $p<0.05$), with the exception of GLCM energy ($p=0.115$) (**Table 2**). Post-hoc
178 pairwise comparisons demonstrated that across each image resolution, muscle composition
179 features displayed heterogeneous differences depending on the feature and image resolution
180 evaluated (**Table 2**).

181 Across all image resolutions, kurtosis, histogram energy, and GLCM contrast displayed
182 moderate-to-good/excellent ICC scores, whereas the remaining features displayed poor-to-
183 moderate/good agreement (**Table 3**). Generally, the lowest resolution image (9.0 cm imaging
184 depth) revealed the poorest agreement with other imaging depths (ICC ranges 0.087 – 0.794);
185 whereas agreement amongst the higher resolution images (7.3, 5.9, and 4.7 cm imaging depths)
186 was stronger (ICC ranges 0.377 – 0.992). Interestingly, the first order histogram features
187 displayed stronger agreement (ICC ranges 0.894 – 0.992) amongst the higher resolution images
188 compared with second and higher order texture features (ICC ranges 0.377 – 0.934) (**Table 3**).

189 **DISCUSSION**

190 In the current study, we show that ultrasound image resolution, which is altered by
191 scanning depth, significantly influences texture analysis of skeletal muscle tissue. For all muscle
192 composition texture features, we observed a wide range of agreement (from poor to excellent)
193 amongst the various image resolutions. In general, higher resolution images displayed better
194 agreement compared to lower resolution images, indicating the importance of accounting for
195 image depth between and within participants when evaluating muscle composition.

Surrogates of skeletal muscle composition are increasingly being evaluated using ultrasound (Correa-de-Araujo et al. 2017). Since muscle composition is characterized using image pixel intensities and spatial distributions, several ultrasound equipment settings require standardization to ensure consistency in analysis between and within individuals. Equipment settings such as gain, time-gain-compensation, dynamic range, and manufacturer proprietary settings are known to influence pixel intensities and require standardization (Pillen and van Alfen 2011). Imaging depth is a parameter that is often altered between and within individuals to fully visualize muscles and account for differences in muscle size and subcutaneous adipose tissue thickness. While some studies report the use of a single ultrasound imaging depth for muscle composition analysis (Zaidman et al. 2012, Wilhelm et al. 2014), this is not universally implemented (Young et al. 2015, Minetto et al. 2016). Because the influence of ultrasound image resolution on analysis of skeletal muscle composition is not well understood, interpretation of muscle composition across different imaging depths can be challenging.

To our knowledge, only one other study has evaluated the influence of ultrasound image resolution (at depths of 2.46, 3.71, and 4.93 cm) on texture characterization, however, this was performed on malignant and benign breast lesion scans (Lefebvre et al. 2000) rather than muscle tissue. In this study, Lefebvre et al. (2000) examined 12 different first and second order texture features and observed high coefficients of variation (CVs) between the three image depths: six features displayed CVs greater than 20%, and the remaining six features displayed CVs between 10-20%. These large deviations support our findings and suggest that image resolution has a significant impact on texture analysis. However, we observed better agreement between the higher resolution scans (at depths of 7.3, 5.9 and 4.7 cm), whereas, Lefebvre et al. (2000) observed poor agreement even at relatively shallow imaging depths (i.e. higher resolution scans)

(Lefebvre et al. 2000). This discrepancy between the current study at Lefebvre et al. (2000) may be due to differences in image resolution (i.e. cm/pixel) across different ultrasound manufacturers, rather than specific imaging depths (i.e. cm). In future analyses, it may be useful to report both image resolution and depth, to assist readers with interpretation and comparison of muscle composition analysis.

When comparing ICC's across different texture features, first order analyses (e.g. echo intensity, histogram kurtosis, and histogram energy) exhibited the highest degree of agreement for higher resolution images (image depths 7.3, 5.9, and 4.7 cm). Given the technical nature of measurement and interpretation of second and higher order texture features, it may be that 1st order texture features are sufficient for describing muscle composition. However, our analysis solely evaluated agreement between different image resolutions. Additional analyses are needed to evaluate which of these texture features are most useful for characterizing muscle composition relative to reference measures of intramuscular adipose tissue (e.g. magnetic resonance imaging).

Given the influence of image resolution on texture features, it is critical for researchers to select a single, fixed depth with a high image resolution when analyzing muscle composition between and within participants in a single study. In our young healthy cohort, a depth of 4.7 cm fully captured the cross-sectional area of the rectus femoris at our landmark (the lower 2/3 of the anterior thigh) in 97% of our participants. However, due to our relatively small sample size and lack of participants with higher BMIs (and likely greater thigh circumferences and/or subcutaneous adipose tissue thickness), 4.7 cm may not be deep enough to capture the entire rectus femoris cross-sectional area in all individuals of a more heterogeneous cohort. Therefore, at the lower 2/3 anterior thigh landmark and with our equipment, a depth of ~6.0 cm may better capture the entire rectus femoris and be more appropriate for muscle composition analysis.

242 However, it should be noted that this depth will likely be insufficient to capture the femur within
243 the field of view for all participants, limiting concurrent analysis of muscle thickness and
244 composition. Furthermore, since image resolution and scanning depth are unique to each
245 ultrasound and transducer combination, we recommend that researchers familiarize themselves
246 with the capabilities and limitations of their equipment to ensure consistency within a study.

247 A limitation of the current study is that our participant cohort consisted solely of
248 apparently healthy younger adults. It is unknown whether image resolution has a similar
249 influence on skeletal muscle from older adults or clinical populations, who tend to present with
250 poorer muscle composition (Strasser et al. 2013). Furthermore, we only evaluated the agreement
251 of muscle composition across different image resolutions, thus the usefulness of specific texture
252 features in differentiating individuals with good or poor muscle composition requires further
253 investigation. This limitation is particularly important for determining if the differences due to
254 image resolution represents a clinically meaningful change, rather than just a statistically
255 significant difference. For example, our previous work has shown that the mean difference in
256 rectus femoris echo intensity between older and younger adults is 15.1 arbitrary units (Paris et al.
257 2017). The 3.0 unit difference in echo intensity between depths of 7.3 and 4.7 cm is statistically
258 significant, but may not be clinically meaningful. However, the 13.1 unit difference between 9.0
259 and 4.7 cm would represent a clinically meaningful influence. Lastly, the exact depths and image
260 resolutions used in this study may not be reproducible on other ultrasound devices, limiting
261 direct comparisons with our findings and further supporting the need for intra-study report of
262 depth analysis.

263 In conclusion, our study demonstrates that ultrasound image resolution significantly
264 influences analysis of skeletal muscle composition. The depth of ultrasound imaging should be

held constant (or at least accounted for) between and within participants to ensure comparable measurements are obtained.

Acknowledgements

This work was supported by grants from the University of Waterloo's Network for Aging Research.

Conflicts of interest

The authors have no conflicts of interest to disclose.

REFERENCES

Cadore EL, Izquierdo M, Conceição M, *et al.* Echo intensity is associated with skeletal muscle power and cardiovascular performance in elderly men. *Exp. Gerontol.* (2012); **47**: 473–8.

Caresio C, Molinari F, Emanuel G, *et al.* Muscle echo intensity: reliability and conditioning factors. *Clin. Physiol. Funct. Imaging* (2014); **5**: 393–403.

Castellano G, Bonilha L, Li LM, *et al.* Texture analysis of medical images. *Clin. Radiol.* (2004); **59**: 1061–1069.

Correa-de-Araujo R, Harris-Love MO, Miljkovic I, *et al.* The Need for Standardized Assessment of Muscle Quality in Skeletal Muscle Function Deficit and Other Aging-Related Muscle Dysfunctions: A Symposium Report. *Front. Physiol.* (2017); **8**: 1–19.

Frank-Wilson AW, Chalhoub D, Figueiredo P, *et al.* Associations of Quadriceps Torque Properties with Muscle Size, Attenuation, and Intra-Muscular Adipose Tissue in Older Adults. *J. Gerontol. A. Biol. Sci. Med. Sci.* (2018); **7**: 931–938.

285 Goodpaster BH, Carlson CL, Visser M, *et al.* Attenuation of skeletal muscle and strength in the
286 elderly: The Health ABC Study. *J. Appl. Physiol.* (2001); **90**: 2157–2165.

287 Goodpaster BH, Park SW, Harris TB, *et al.* The loss of skeletal muscle strength, mass, and
288 quality in older adults: the health, aging and body composition study. *J. Gerontol. A. Biol.*
289 *Sci. Med. Sci.* (2006); **61**: 1059–64.

290 Hall-beyer M. Practical guidelines for choosing GLCM textures to use in landscape classification
291 tasks over a range of moderate spatial scales. *Int. J. Remote Sens.* (2017); **38**: 1312–1338.

292 Harris-Love MO, Monfaredi R, Ismail C, *et al.* Quantitative ultrasound: Measurement
293 considerations for the assessment of muscular dystrophy and sarcopenia. *Front. Aging*
294 *Neurosci.* (2014); **6**: 1–4.

295 König T, Steffen J, Rak M, *et al.* Ultrasound texture-based CAD system for detecting
296 neuromuscular diseases. *Int. J. Comput. Assist. Radiol. Surg.* (2015); **10**: 1493–1503.

297 Koo TK, Li MY. A Guideline of Selecting and Reporting Intraclass Correlation Coefficients for
298 Reliability Research. *J. Chiropr. Med.* (2016); **15**: 155–163.

299 Lefebvre F, Meunier M, Thibault F, *et al.* Computerized ultrasound B-scan characterization of
300 breast nodules. *Ultrasound Med. Biol.* (2000); **26**: 1421–1428.

301 Minetto MA, Caresio C, Menapace T, *et al.* Ultrasound-Based Detection of Low Muscle Mass
302 for Diagnosis of Sarcopenia in Older Adults. *PM R* (2016); **8**: 453–462.

303 Mitchell WK, Williams J, Atherton P, *et al.* Sarcopenia, dynapenia, and the impact of advancing
304 age on human skeletal muscle size and strength; a quantitative review. *Front. Physiol.*
305 (2012); **3**: 1–18.

306 Molinari F, Caresio C, Acharya UR, *et al.* Advances in Quantitative Muscle Ultrasonography
307 Using Texture Analysis of Ultrasound Images. *Ultrasound Med. Biol.* (2015); **41**: 2520–
308 2532.

309 Paris, Mourtzakis M. Assessment of skeletal muscle mass in critically ill patients: considerations
310 for the utility of computed tomography imaging and ultrasonography. *Curr. Opin. Clin.*
311 *Nutr. Metab. Care* (2016); **19**: 125–130.

312 Paris MT, Lafleur B, Dubin JA, *et al.* Development of a bedside viable ultrasound protocol to
313 quantify appendicular lean tissue mass. *J. Cachexia. Sarcopenia Muscle* (2017); **8**: 713–
314 726.

315 Parry SM, El-Ansary D, Cartwright MS, *et al.* Ultrasonography in the intensive care setting can
316 be used to detect changes in the quality and quantity of muscle and is related to muscle
317 strength and function. *J. Crit. Care* (2015); **30**: 1151.e9-1151.e14.

318 Pillen S, van Alfen N. Skeletal muscle ultrasound. *Neurol. Res.* (2011); **33**: 1016–1024.

319 Rech A, Radaelli R, Goltz FR, *et al.* Echo intensity is negatively associated with functional
320 capacity in older women. *Age (Omaha).* (2014); **36**: 1–9.

321 Strasser EM, Draskovits T, Praschak M, *et al.* Association between ultrasound measurements of
322 muscle thickness, pennation angle, echogenicity and skeletal muscle strength in the elderly.
323 *Age* (2013); **35**: 2377–2388.

324 Visser M, Goodpaster BH, Kritchevsky SB, *et al.* Muscle mass, muscle strength, and muscle fat
325 infiltration as predictors of incident mobility limitations in well-functioning older persons.
326 *J. Gerontol. A. Biol. Sci. Med. Sci.* (2005); **60**: 324–333.

Wilhelm EN, Rech A, Minozzo F, *et al.* Relationship between quadriceps femoris echo intensity, muscle power, and functional capacity of older men. *Age (Omaha).* (2014); **36**: 1113–1122.

Young H-J, Jenkins NT, Zhao Q, *et al.* Measurement of intramuscular fat by muscle echo intensity. *Muscle and Nerve* (2015); **52**: 963–71.

Zaidman CM, Holland MR, Hughes MS. Quantitative Ultrasound of Skeletal Muscle: Reliable Measurements of Calibrated Muscle Backscatter from Different Ultrasound Systems. *Ultrasound Med. Biol.* (2012); **38**: 1618–1625.

Figure 1

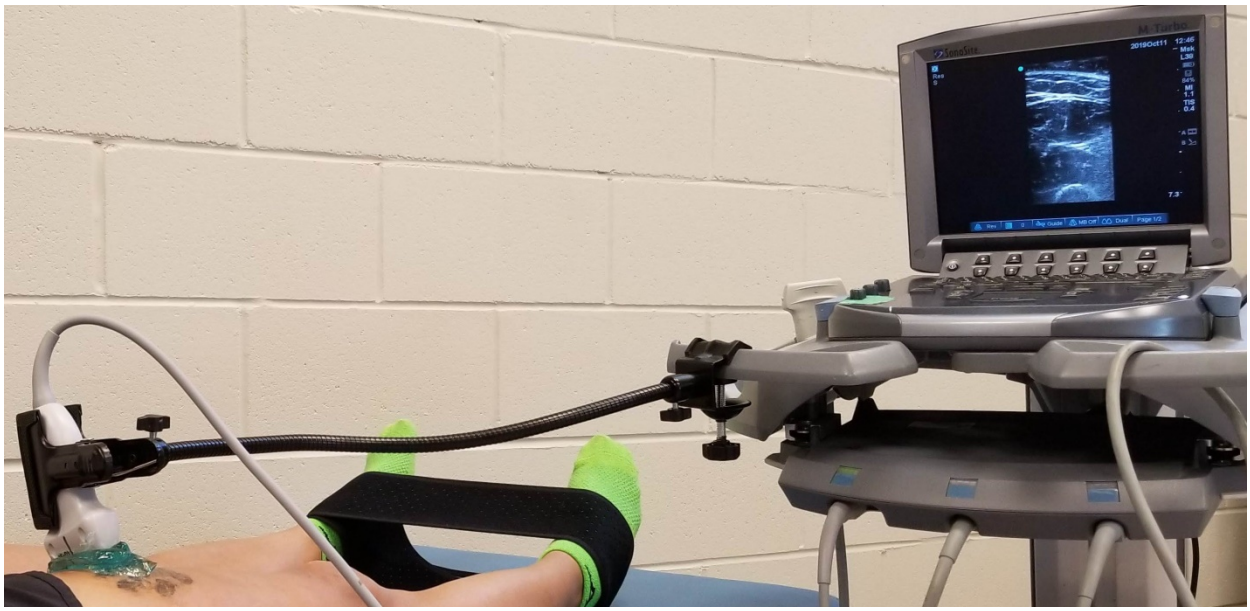

337 **Figure 2**

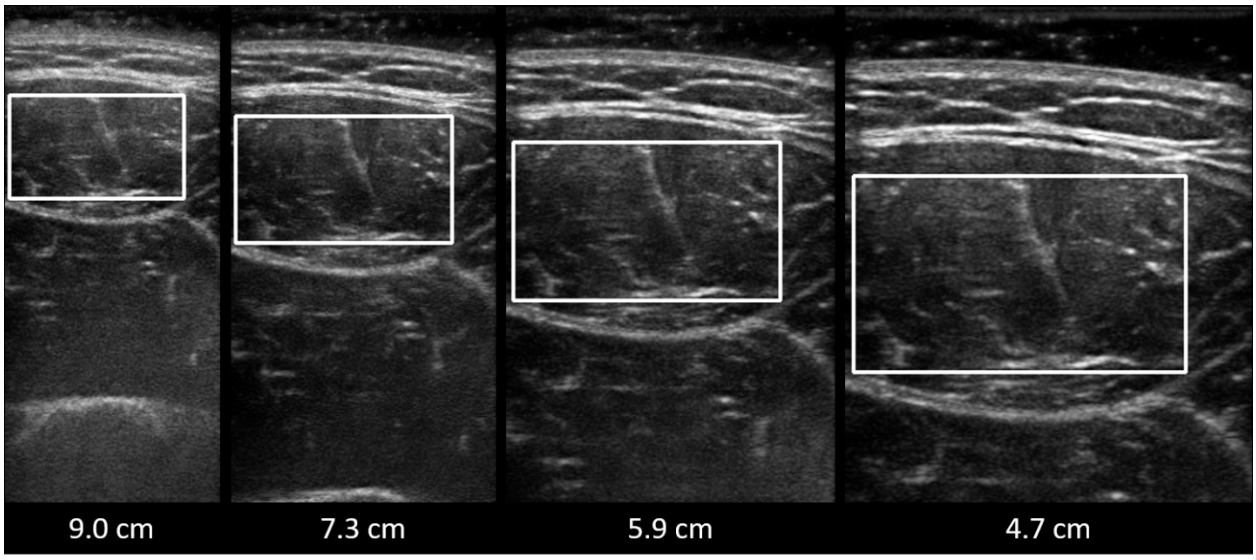

338

Figure captions list

Figure 1. Transducer apparatus. Once the correct medial-lateral and cranial-caudal orientations were achieved, and minimal tissue compression was confirmed, the transducer was fixed in place with flexible gooseneck clamp. This position was maintained while transverse images of the thigh were captured at discrete depths of 9.0, 7.3, 5.9, and 4.7 cm.

Figure 2. Automatic region of interest selection across different image resolutions. The region of interest was manually selected in the 9.0 cm depth image and automatically scaled to the remaining images.

348 **Table 1.** Demographic and physical characteristics.

	All (n=32)	Males (n=16)	Females (n=16)	p-value
Age, years	28 ± 5	27 ± 3	28 ± 7	0.315
Weight, kg	70.6 ± 13.0	78.3 ± 10.9	63.0 ± 10.7	<0.001
Height, m	1.70 ± 0.07	1.74 ± 0.05	1.66 ± 0.06	<0.001
BMI, kg/m^2	24.4 ± 3.4	25.8 ± 3.3	22.9 ± 3.0	0.011
Right leg dominant, n	27	13	14	-
Muscle thickness, cm	3.97 ± 0.86	4.61 ± 0.62	3.36 ± 0.61	<0.001
Adipose tissue thickness, cm	0.91 ± 0.56	0.64 ± 0.39	1.19 ± 0.59	0.004
Minimum imaging depth, cm	5.9	4.7	5.9	-

349 Data are presented as mean ± SD
350 Minimum imaging depth refers to depth required to fully visualize the inferior fascia of the
351 rectus femoris
352 Abbreviations: BMI, body mass index.

353

354

Table 2. Comparison of muscle texture features between different resolution images

Image depth	9.0 cm (n=32)	7.3 cm (n=32)	5.9 cm (n=32)	4.7 cm (n=31)	ANOVA p-value
Echo intensity	52.9 ± 9.0^{a}	42.8 ± 7.1^{b}	40.6 ± 7.7^{c}	39.8 ± 7.9^{d}	<0.001
Histogram kurtosis	2.42 ± 1.65^{a}	3.57 ± 3.31^{ab}	3.97 ± 3.16^{b}	4.08 ± 3.36^{b}	0.001
Histogram energy	0.130 ± 0.011^{a}	0.135 ± 0.014^{b}	0.137 ± 0.012^{c}	0.134 ± 0.014^{b}	<0.001
GLCM energy	0.025 ± 0.007	0.023 ± 0.003	0.023 ± 0.003	0.022 ± 0.003	0.115
GLCM contrast	304.5 ± 161.8^{ab}	311.1 ± 95.4^{a}	329.0 ± 99.0^{b}	370.4 ± 120.9^{c}	<0.001
GLCM correlation	0.63 ± 0.09^{a}	0.57 ± 0.08^{b}	0.53 ± 0.08^{c}	0.51 ± 0.10^{d}	<0.001
LBP energy	0.168 ± 0.007^{ab}	0.169 ± 0.005^{a}	0.165 ± 0.005^{b}	0.164 ± 0.005^{b}	<0.001

Data are presented in arbitrary units as mean ± SD.
Within each row, values that do not share a letter are statistically dissimilar.
First order features: echo intensity, histogram kurtosis, histogram energy; second order features: GLCM energy, GLCM contrast, GLCM correlation; higher order feature: LBP energy.
Corresponding depths and image resolutions: 9.0 cm – 0.0234 cm/pixel, 7.3 cm – 0.0189 cm/pixel, 5.9 cm – 0.0153 cm/pixel, 4.7 cm – 0.0123 cm/pixel.
Abbreviations: ANOVA, analysis of variance; GLCM, grey-level co-occurrence matrix; LBP, local binary pattern.

Table 3. Intraclass correlation coefficients across different image resolutions.

	All	9.0 vs 7.3 cm	9.0 vs 5.9 cm	9.0 vs 4.7 cm	7.3 vs 5.9 cm	7.3 vs 4.7 cm	5.9 vs 4.7 cm
Echo intensity	0.606 (0.120, 0.839)	0.492 (-0.066, 0.825)	0.467 (-0.016, 0.825)	0.450 (-0.012, 0.817)	**0.919** (0.546, 0.974)	0.894 (0.284, 0.969)	**0.992** (0.962, 0.997)
Histogram kurtosis	0.750 (0.592, 0.861)	0.427 (0.111, 0.669)	0.481 (0.108, 0.723)	0.474 (0.098, 0.720)	**0.941** (0.878, 0.972)	**0.935** (0.853, 0.970)	**0.988** (0.974, 0.994)
Histogram energy	0.844 (0.698, 0.922)	0.706 (0.393, 0.858)	0.724 (0.007, 0.908)	0.794 (0.497, 0.909)	**0.927** (0.824, 0.967)	**0.945** (0.889, 0.973)	**0.949** (0.681, 0.984)
GLCM energy	0.373 (0.196, 0.572)	0.283 (-0.053, 0.566)	0.183 (-0.159, 0.491)	0.190 (-0.144, 0.495)	**0.909** (0.821, 0.954)	0.874 (0.756, 0.937)	0.883 (0.765, 0.943)
GLCM contrast	0.696 (0.540, 0.822)	0.572 (0.281, 0.766)	0.600 (0.328, 0.782)	0.592 (0.273, 0.787)	**0.934** (0.824, 0.971)	0.807 (0.059, 0.941)	0.876 (0.362, 0.960)
GLCM correlation	0.595 (0.175, 0.817)	0.726 (-0.069, 0.921)	0.469 (-0.077, 0.807)	0.390 (-0.079, 0.752)	0.818 (0.003, 0.949)	0.717 (-0.072, 0.921)	0.813 (0.597, 0.912)
LBP energy	0.430 (0.243, 0.625)	0.546 (0.246, 0.750)	0.371 (0.052, 0.627)	0.087 (-0.199, 0.390)	0.638 (0.114, 0.847)	0.377 (-0.038, 0.668)	0.746 (0.525, 0.871)

All data are presented in arbitrary units as ICC (95% CI).
Comparisons with excellent agreement (ICC > 0.90) are bolded.
First order features: echo intensity, histogram kurtosis, histogram energy; second order features: GLCM energy, GLCM contrast, GLCM correlation; higher order feature: LBP energy.
Corresponding depths and image resolutions: 9.0 cm – 0.0234 cm/pixel, 7.3 cm – 0.0189 cm/pixel, 5.9 cm – 0.0153 cm/pixel, 4.7 cm – 0.0123

cm/pixel.
Abbreviations: GLCM, grey-level co-occurrence matrix; ICC, intraclass correlation coefficient; LBP, local binary pattern.